FOREX Publication
Open Access | Rapid and quality publishing

International Journal of
Electrical and Electronics Research (IJEER)
Research Article | Volume 10, Issue 4 | Pages 1154-1158 | e-ISSN: 2347-470X

Performance Improvement of Induction Motor Controlled by Thyristor Chopper on the Rotor Side

Bilal Abdullah Nasir*
Department of Electrical Technologies, Northern Technical University, Iraq

***Correspondence:** Bilal Abdullah Nasir; bilalalnasir@ntu.edu.iq

ABSTRACT- In this paper, the performance characteristics of a variable-speed drive system with a wound rotor induction motor incorporating a 3-phase diode bridge rectifier - thyristor chopper with a modified commutation circuit system on the rotor side were studied. A DC equivalent circuit was used in the analysis of the motor-rectifier-chopper system and suitable equations have been derived for the determination of the system performance. The analytical results obtained are compared with those obtained experimentally to ascertain the validity of the system in practical applications. The results obtained indicate that a true variable speed drive system based on a thyristor chopper-controlled induction motor is successfully implemented. It is shown that the thyristor chopper control using the Hitachi commutation circuit permits the realization of a slip-ring induction motor as a variable speed and improved power factor. Also, the torque level obtained by the chopper control was found to be three times that obtained from conventional rotor resistance control at the same conditions.

Keywords: Wound rotor induction motor, thyristor chopper, bridge-rectifier, duty-ratio.

ARTICLE INFORMATION
Author(s): Bilal Abdullah Nasir;
Received: 20/08/2022; **Accepted**: 08/12/2022; **Published**: 20/12/2022;
e-ISSN: 2347-470X;
Paper Id: IJEER 2008-29;
Citation: 10.37391/IJEER.100463
Webpage-link:
www.ijeer.forexjournal.co.in/archive/volume-10/ijeer-100463.html

Publisher's Note: FOREX Publication stays neutral with regard to Jurisdictional claims in Published maps and institutional affiliations.

1. INTRODUCTION

With the commercial availability of thyristors of medium and high-power ratings, static power conversion techniques have increasingly been used for speed control of induction motors because of their large power handling capacity, compact size, reliability, and ease of control [1,2].

The use of thyristor switches for control of stator voltage is restricted to small-size motors only [1]. For control of induction motors, especially of medium and large sizes, the air-gap flux must be constant. In the rotor control, the stator voltage and frequency are kept constant, therefore, the control of the rotor currents to obtain variable speed is preferred [2-6].

The chopper chopped the rotor current at different instants to get variable torque-speed characteristics. The works in [7-10] were limited to some extent regarding the range of the chopping frequency and the speed. The present work is based on the same thyristor chopper system but the commutation circuit of the chopper is replaced by a circuit model called the Hitachi commutation (resonance) circuit used in the analysis of the motor-rectifier-thyristor chopper system, which permits a wide range of chopping frequency and speed variation, to get improved performance, such as high motor torque and power factor.

Different practical cases are studied, such as varying the chopping frequency and keeping the duty ratio of the DC chopper constant and vice versa. Theoretical results from the model have been verified and compared with the experimental results to show the validity of the present work for the performance determination of the motor when controlled from the rotor side. The following sections deal with the analysis of the motor-chopper system, the experimental study, and the conclusions.

2. THE RECTIFIER-CHOPPER SYSTEM

The complete system used in the rotor side of the motor is shown in *figure 1*, which consists of two main parts, a three-phase bridge diode rectifier and a thyristor switch as a chopper. The rectifier rectifies the AC rotor voltage while the chopper controls the resistance effectively connected to the rotor by the switching action of the chopper.

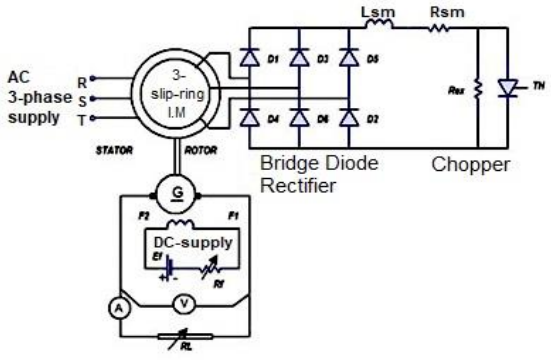

Figure 1: The complete motor-bridge rectifier-thyristor chopper system

2.1 The Rectifier Circuit

The rectifier circuit is a three-phase bridge diode rectifier [11]. It converts the rotor AC voltage into DC and then it is fed to the

FOREX Publication
Open Access | Rapid and quality publishing
International Journal of Electrical and Electronics Research (IJEER)
Research Article | Volume 10, Issue 4 | Pages 1154-1158 | e-ISSN: 2347-470X

DC chopper. The output DC voltage of the rectifier is given as [11]-[14]:

$$V_d = S(3\sqrt{6})E`_1/\pi \quad (1)$$

Where $E`_1 = (V_L/\sqrt{3})/(N_1/N_2)$ is the stator phase voltage (r.m.s) referred to the rotor side, V_L is the line supply voltage (r.m.s), (N_1/N_2) is the stator to rotor winding ratio, and (S) is the motor slip.

2.2 The Chopper Circuit

The chopper circuit connected to the rotor external resistance (Rex) is shown in *figure 1*. It consists of a thyristor (TH) and its commutating circuit. The commutation circuit is used to provide a very wide range of chopping frequencies. It consists of the main thyristor denoted Tm, an auxiliary thyristor denoted Ta and two diodes denoted D7 and D8, along with a resonance circuit consisting of inductor L and capacitor C, as shown in *figure 2*.

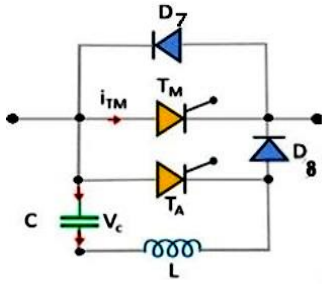

Figure 2: Hitachi commutation circuit of the thyristor chopper

The operation and analysis of the chopper circuit are presented and explained in detail in references [9-10] under the following assumptions:

a. The thyristors are perfect and identical switches.
b. The reverse recovery voltage of the thyristor is instantaneous.
c. The resonance circuit of the commutation circuit (L-C) is lossless.

Due to a small leakage inductance in the rotor circuit, the time constant during the ON/OFF periods is very small. Hence, the current reaches a steady state quickly and so the rotor winding currents may become discontinuous. This high rate of change of current produces voltage pulses across the thyristor-chopper. This problem was solved by introducing a smoothing inductance (Ls) in the rotor circuit [12], as shown in *figure 1*. The inductance (Ls) is desirable to limit the ripple of current flow in the D.C. link between the diode bridge rectifier and chopper. This inductance makes the rotor current continuous.

3. THE CHOPPING FREQUENCY

There are some important points regarding the selection of the chopper frequency, as follows [10]:

1. With higher values of chopping frequency, the size of smoothing inductance can be minimized and the motor vibration is also reduced.
2. A very high value of the chopping frequency increases the failure probability of commutation, due to the finite minimum ON and OFF times of the thyristor. The minimum and maximum width of both ON and OFF periods are therefore defined in this case between (40 - 1.67) msec, which corresponds to a chopping frequency between (25-600) Hz.

4. ANALYSIS OF THE MOTOR-CHOPPER SYSTEM

4.1 The System Description

The schematic diagram of the slip-ring induction motor-chopper system is shown in *figure 1*. The induction motor is fed from a standard 3-phase mains supply. A 3-phase bridge diode rectifier is connected to the rotor slip-ring terminals, and the output is fed to the chopper circuit through the smoothing inductor and external resistance (Rex). Due to the presence of the chopper in the rotor, an effective resistance (Ref), which depends on the duty cycle ratio (γ), will appear across the bridge terminals.

The duty ratio (γ) depends on the control circuit. If no gate signals are given to the thyristors, almost no current flows in the rotor circuit, because of the highly effective rotor resistance. This condition is equivalent to that of an open circuit rotor and no torque is developed. If the thyristors are triggered the current will flow in the rotor circuit. This current is controlled by varying the conduction period of the thyristors. When the thyristors are allowed about full conduction (γ =1.0), the D.C. side resistance will be minimal due to the effective resistance (Ref = (1- γ) Rex) being zero. This condition is almost equivalent to that of the short-circuited rotor [10]. Thus, the rotor current and motor torque are controlled from a minimum to maximum value and the motor speed will vary too.

4.2 Steady-State Model

For the formulation of machine equations, the thyristor operation is assumed to be an ideal switch.

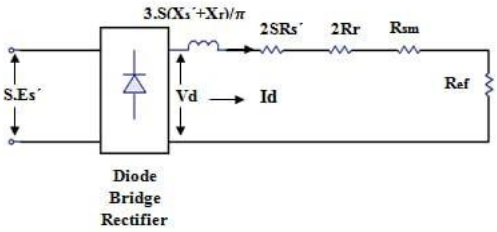

Figure 3: The system equivalent circuit model transferred to the rotor side

Figure 3 shows the system equivalent circuit model with all quantities transferred to the rotor side, and the equivalent circuit parameters are given in appendix-A. The rotor current is approximately composed of alternating square pulses of (2π /3) duration [12]. The average rectified current (I_d) is related to the rotor r.m.s. phase current I_r by:

$$I_r = \sqrt{\frac{2}{3}} I_d \quad \text{or} \quad I_r^2 = \frac{2}{3} I_d^2 \quad (2)$$

FOREX Publication
Open Access | Rapid and quality publishing
International Journal of Electrical and Electronics Research (IJEER)
Research Article | Volume 10, Issue 4 | Pages 1154-1158 | e-ISSN: 2347-470X

The total copper losses in the stator and rotor resistances (P_{cu}) of the three phases are calculated from the system equivalent circuit and *equation 2* above, as:

$$P_{cu} = 3I_r^2 (SR_s` + R_r) = 2\, I_d^2 (SR_s` + R_r) \quad (3)$$

Hence the term $3(SR_s`+R_r)$ transferred across the rectifier bridge, appears as $2(SR_s`+R_r)$ on the D.C. side. Due to the leakage reactance ($S.X_s`$) and ($S.X_r$), the commutation of current between the bridge diodes is no longer instantaneous. There is a period of current overlap where two phases carry current simultaneously. This causes a voltage reduction (V_{dr}) from the terminals of the rectifier bridge, which is given as [1]:

$$V_{dr} = 3S(X_s` + X_r)\, I_d / 2\pi \quad (4)$$

Therefore, from the equivalent circuit of *figure 2*, the DC (I_d) is obtained as [1]:

$$I_d = \frac{V_d}{\left[\frac{3S(X_s`+X_r)}{\pi} + 2(SR_s`+R_r) + R_{sm} + R_{ef}\right]} \quad (5)$$

Where (R_{sm}) is the resistance of the smoothing inductor, and R_{ef} is the effective external rotor resistance, which is given as [10]:

$$R_{ef} = (1-\gamma)\, R_{ex} \quad (6)$$

By adjusting the parameter (γ) in the range ($0<\gamma<1.0$), the effective resistance R_{ef} will vary in the range ($0<R_{ef}<R_{ex}$).

From the DC equivalent circuit, the average output power (P_{av}) of the rectifier is calculated as:

$$P_{av.} = I_d^2 (2R_r + R_{sm} + R_{ef}) \quad (7)$$

This power represents the copper loss in the rotor circuit.

But the mechanical output power is given as [10]:

$$P_m = \frac{Rotor\ copper\ loss}{S} \quad (8)$$

Also, the mechanical power is given as [10]:

$$P_m = T_m . W_S \quad (9)$$

Where T_m is the mechanically developed torque and W_s is the synchronous speed in radian/sec.

From *equations (8) and (9)* the developed mechanical torque can be drived as:

$$T_m = I_d^2 \frac{(2R_r + R_{sm} + R_{ef})}{SW_S} \quad (10)$$

The practical mechanical torque is measured by the torque meter or by using the relation [11]:

$$T_m = \frac{P_{out}}{(2\pi N_r/60)} \quad (11)$$

Where Pout is the output power of the motor (watts) and N_r is the rotor speed (r.p.m).

5. RESULTS AND DISCUSSION

A laboratory experimental set-up is introduced to study and verify the performance characteristics of the motor-thyristor chopper system and a comparison between the practical and theoretical results is presented. At the same time, a comparison is made between the chopper controls systems investigated in this work with the conventional rotor resistance control method. The test 3-phase induction motor is directly coupled to a separately excited DC generator as a load, as shown in *figure 1*.

Details of the induction motor system, as well as the DC machine are given in appendices A and B. The trigger control signals of the thyristors are obtained from a thyristor board. The characteristics obtained experimentally and theoretically are presented together in the same figures to facilitate visual comparison of the predicted and experimental results.

The performance characteristics for γ = 0.8 and chopping frequency range from (25-600) Hz are presented. *Figure 4* shows the theoretical and practical results of torque-speed characteristics under the same conditions. As the value of frequency decreases, the torque level decreases too. The corresponding characteristics of the conventional rotor resistance control at a constant value (R_r=37) are shown in the same figure. It is similar in shape to the chopper control but much lower torque level. *Figure 5* shows the power factor-speed characteristics for γ = 0.8. The power factor is improved by increasing the chopping frequency. The characteristics are identical in shape to that obtained from the conventional rotor resistance control, which is shown in the same figure, except that in the chopper control method the power factor is improved by more than 50%.

Figures 6 and *7* show the torque-speed and power factor-speed characteristics, respectively, for variable duty ratio (γ =0.05 to 0.95) and fixed chopping frequency at (25) Hz. The torque and power factor become higher for higher values γ, due to the reduction in the effective rotor resistance.

The duty ratio parameter (γ) is limited between 0.05 to 0.95 and the chopping frequency is between (25-600) Hz. The limitation of the duty ratio is due to the commutation time loss which is high at high frequencies. The general performance of the system within the limits is improved at high values of γ and chopping frequency. The experimental readings are slightly different from the theoretical calculations due to the assumptions imposed in the analysis. The close agreement between the predicted and measured results confirms the validity of the analysis.

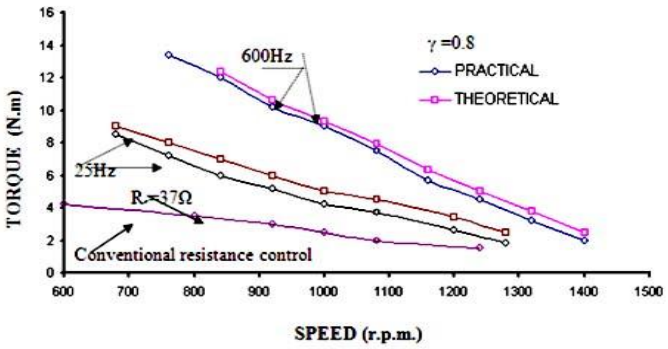

Figure 4: Torque-speed variation at the different chopping frequencies

FOREX Publication
Open Access | Rapid and quality publishing
International Journal of Electrical and Electronics Research (IJEER)
Research Article | Volume 10, Issue 4 | Pages 1154-1158 | e-ISSN: 2347-470X

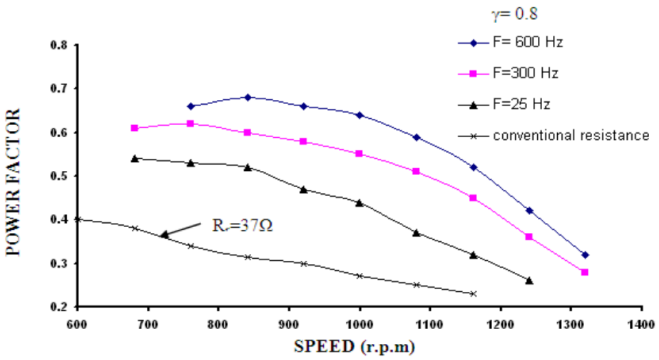

Figure 5: Power factor-speed variation at the different chopping frequency

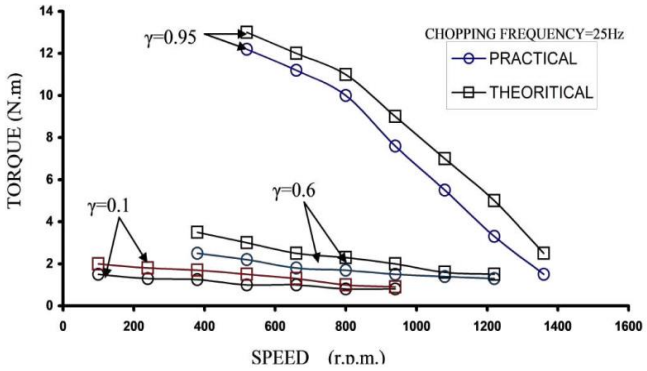

Figure 6: Torque-speed variation at different duty cycle ratios

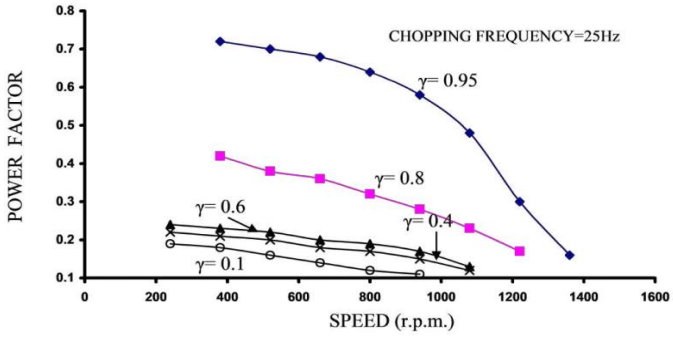

Figure 7: Power factor-speed variation at different duty cycle ratios

6. CONCLUSION

The implemented speed control drive system was found to give a smooth and wide range of speed control under various loading conditions. The obtained torque level by the thyristor chopper control with the Hitachi resonance commutation circuit was found to be approximately three times that obtained by the conventional rotor resistance method at the same conditions. According to the results, also, the input power factor is considerably improved by more than 50% compared with that obtained by the conventional rotor resistance control method under the same conditions.

APPENDICES

A. Details of the induction motor:

3-phase, slip-ring, Y-Y connection, 50 Hz

Stator	rotor
380 V	120 V
4.5 A	10 A

Stator/rotor turns ratio (N_1/N_2) = 3.16
Output power = 1.8 Kw, full load speed = 1390 r.p.m

The per-phase parameters of the motor equivalent circuit transferred to the rotor side, except for Xm, are:

$R_s^{`}$= stator resistance = 0.435 Ω
$X_s^{`}$= stator leakage reactance = 0.69 Ω
R_r = rotor resistance = 0.314 Ω
X_r = rotor leakage reactance = 0.501 Ω
X_m = magnetizing reactance = 99.1 Ω
R_{ex} = external rotor resistance = 175 Ω

B. Details of DC Generator

Type: ASIA company machine

Rated speed = 1250 r.p.m
Rated power = 2.3 kW
Rated current = 13 A
Rated Voltage = 220 V
Armature resistance = 4.8Ω. The rotational losses of the D.C. machine at constant flux are obtained from Swinburne's test. The relation between rotational losses and armature speed (Nr) is obtained as:

$$\text{Rotational losses} = 25 + \frac{36}{300}(\text{Nr}-400) \text{ watts}$$

REFERENCES

[1] Paresh, C. sen, and Ma, K.H.J. 1975. Rotor chopper control for induction motor drive. IEEE Trans. IA, Vol. IA-11, No. 1, pp.43-49. DOI: 10.1109/TIA.1975.349256

[2] Wani, N.S. and Ramamoorthy, M. 1977. Chopper Controlled Slipring Induction Motor. IEEE Transactions on Industrial Electronics and Control Instrumentation, Vol. IECI-24, Issue. 2, pp. 153-161. DOI: 10.1109/TIECI.1977.351457

[3] Sen, P.C. 2014. Principles of electric machines and power electronics. John Wiley and Sons, New York. https://www.wiley.com/enus/Principles+of+Electric+Machines+and+Power+Electronics%2C+3rd+Edition-p-9781118078877.

[4] Wani, N.S. and Ramamoorthy, M. 1977. Chopper-controlled slip ring induction motor. IEEE Trans. on Industrial Electronics and Control Instrumentation, Vol. IECI-24, No. 2, pp.153-161. http://www.irphouse.com/ijee/ijeev5n2_08.pdf

[5] Chin, S. Moo, Chung, C. Wei, Ching, L. Huang, Chao S. C. 1989. Starting control of the Wound rotor induction motor by using chopper-controlled Resistance in the rotor circuit. Proceedings of IEEE, pp. 2295-2300. DOI: 10.1109/IAS.1989.96962

[6] Dr. Saeed Lesan, Dr. Mohamed S.Smiai, and Prof. William shepherd. 1996. Control of Wound Rotor Induction motor using thyristor in the secondary circuits. IEEE Trans., pp.380-389. DOI: 10.1109/28.491482.

[7] Sang-UK, Jin-ho Choi, Bo -youl. Kim, and Young-Seok Km. 2001. Optimal Steady-state performance of induction motor drives. in Proc. ICPE 01, Seoul, pp.428-433. https://www.koreascience.or.kr/article/CFKO200104704081840.pdf

[8] Constantin, S. Mohan, K. Peter, H. and Wilibald, S. 2002. Performance Enhancement of an induction motor with secondary impedance control. IEEE Transactions on Energy Conversion, Vol 7, No.2, pp. 211 – 216. DOI: 10.1109/TEC.2002.1009470

International Journal of
Electrical and Electronics Research (IJEER)
Research Article | Volume 10, Issue 4 | Pages 1154-1158 | e-ISSN: 2347-470X

[9] Abdelfattah, M.Y. 2003. Speed control of wound rotor induction motors using chopper-controlled external resistance enhanced with a dc capacitor. Alexandria Engineering Journal, Vol. 42, No.1, 2003, pp. 25-34.

[10] Bose, B.K. 2002. Power Electronics and AC Drives. Englewood Cliffs, NJ: Prentice-Hall. https://eee.sairam.edu.in/wp-content/uploads/sites/6/2019/07/Modern_power_electronics_and_AC_drives.pdf

[11] Ranjith, K. and Palaniswami, S. 2011. Performance enhancement of Wound rotor induction motor by resonating rotor circuit using Fuzzy controller. European Journal of Scientific Research, Vol.52, No. 4, pp. 580-591. http://www.irphouse.com/ijee/ijeev5n2_08.pdf

[12] Yanmei, Y.A.O. 2016. Study of Induction Machines with Rotating Power Electronic Converter. Doctoral Thesis, Stockholm, Sweden. https://www.divaportal.org/smash/get/diva2:1045804/FULLTEXT01.pdf

[13] Zein, A. S. Din, E. I. and El-Sabbe, A. E. 2019. Speed control of 3-phase induction motor using rotor impedance. IOP Conf. Series: Materials Science and Engineering, Vol. 459, 012008, PP. 1-13. doi:10.1088/1757-899X/459/1/012008

[14] Mingyu, W. Dafang, W. Guanglin, D. Hui, W. Xiu, L. and Zexu, X. 2019. Simplified Rotor and Stator Resistance Estimation Method Based on Direct Rotor Flux Identification. Journal of Power Electronics, Vol. 19, No. 3, pp. 751-760. file:///C:/Users/D.Bilal/Downloads/journal_jpe_19-3_29066534.pdf.

[15] Sandhya Kulkarni, Dr. Archana Thosar (2021), Performance Analysis of Permanent Magnet Synchronous Machine due to Winding Failurese. IJEER 9(3), 76-83. DOI: 10.37391/IJEER.0903081.

[16] Arun Eldho Alia and F. T. Josh (2022), Design Analysis of SSD Optimized Speed Controller for BLDC Motor. IJEER 10(3), 529-535. DOI: 10.37391/IJEER.100321.